Received: 21 November 2023 | Revised: 24 January 2024 | Accepted: 30 January 2024

DOI: 10.1111/jne.13373

ORIGINAL ARTICLE

Journal of Neuroendocrinology WILEY

Development and prenatal exposure to androgens alter potassium currents in gonadotropin-releasing hormone neurons from female mice

Jennifer Jaime[1] | R. Anthony DeFazio[2] | Suzanne M. Moenter[1,2,3,4,5]

[1]The Neuroscience Graduate Program, University of Michigan, Ann Arbor, Michigan, USA

[2]Department of Molecular & Integrative Physiology, University of Michigan, Ann Arbor, Michigan, USA

[3]Department of Internal Medicine, University of Michigan, Ann Arbor, Michigan, USA

[4]Department of Obstetrics & Gynecology, University of Michigan, Ann Arbor, Michigan, USA

[5]The Reproductive Sciences Program, University of Michigan, Ann Arbor, Michigan, USA

Correspondence
Suzanne M. Moenter, Department of Molecular & Integrative Physiology, University of Michigan, 7725 Med Sci II, 1137 E. Catherine St., Ann Arbor, MI 48109-5622, USA.
Email: smoenter@umich.edu

Funding information
Eunice Kennedy Shriver National Institute of Child Health and Human Development, Grant/Award Numbers: F31HD110279, R01HD104345, T32HD079342

Abstract

Pulsatile gonadotropin-releasing hormone (GnRH) release is critical for reproduction. Disruptions to GnRH secretion patterns may contribute to polycystic ovary syndrome (PCOS). Prenatally androgenized (PNA) female mice recapitulate many neuroendocrine abnormalities observed in PCOS patients. PNA and development induce changes in spontaneous GnRH neuron firing rate, response to synaptic input, and the afterhyperpolarization potential of the action potential. We hypothesized potassium currents are altered by PNA treatment and/or development. Whole-cell patch-clamp recordings were made of transient and residual potassium currents of GnRH neurons in brain slices from 3-week-old and adult control and PNA females. At 3 weeks of age, PNA treatment increased transient current density versus controls. Development and PNA altered voltage-dependent activation and inactivation of the transient current. In controls, transient current activation and inactivation were depolarized at 3 weeks of age versus in adulthood. In GnRH neurons from 3-week-old mice, transient current activation and inactivation were more depolarized in control than PNA mice. Development and PNA treatment interacted to shift the time-dependence of inactivation and recovery from inactivation. Notably, in cells from adult PNA females, recovery was prolonged compared to all other groups. Activation of the residual current occurred at more depolarized membrane potentials in 3-week-old than adult controls. PNA depolarized activation of the residual current in adults. These findings demonstrate the properties of GnRH neuron potassium currents change during typical development, potentially contributing to puberty, and further suggest PNA treatment may both alter some typical developmental changes and induce additional modifications, which together may underlie aspects of the PNA phenotype. There was not any clinical trial involved in this work.

KEYWORDS
androgens, GnRH, puberty, polycystic ovary syndrome

This is an open access article under the terms of the Creative Commons Attribution-NonCommercial License, which permits use, distribution and reproduction in any medium, provided the original work is properly cited and is not used for commercial purposes.
© 2024 The Authors. *Journal of Neuroendocrinology* published by John Wiley & Sons Ltd on behalf of British Society for Neuroendocrinology.

1 | INTRODUCTION

Gonadotropin-releasing hormone (GnRH) neurons produce the final central output for the control of reproduction. GnRH release occurs in an episodic pattern, termed pulses.[1,2] GnRH acts at the anterior pituitary where low-frequency GnRH pulses favor the secretion of follicle-stimulating hormone (FSH), and high-frequency pulses favor the secretion of luteinizing hormone (LH).[3,4] Disruptions to the secretion patterns of GnRH, LH, and/or FSH result in altered reproductive function.[5–8] Polycystic ovary syndrome (PCOS) is the leading cause of infertility in females.[9] Patients with hyperandrogenemic PCOS have persistent high-frequency LH pulse secretion and relative FSH deficiency,[9–12] suggesting GnRH pulses are also persistently high frequency. Interestingly, PCOS-like symptoms have been observed in peripubertal girls, suggesting the neuroendocrine system is altered even before puberty is complete.[13,14]

The etiology of PCOS remains largely unknown. In addition to possible genetic causes,[15,16] it has been hypothesized that in utero exposure to high circulating levels of androgens from the mother might reprogram the reproductive neuroendocrine system. This postulate has been supported by animal models including non-human primates, rats, sheep, and mice.[17–22] In these models, treatment of pregnant dams with androgens produces offspring that develop neuroendocrine phenotypes similar to those observed in females with hyperandrogenemic PCOS. Adult female prenatally androgenized (PNA) mice exhibit increased circulating testosterone levels, increased LH pulse frequency, and disrupted estrous cycles.[20,22–24] PNA causes early vaginal opening (VO), an external index of pubertal onset,[25] suggesting PNA alters reproductive development. The use of mouse models makes it possible to measure neurophysiologic parameters. Spontaneous GnRH neuron firing rate changes with development in controls and is altered by PNA treatment in both prepubertal and adult mice. Specifically, in PNA females, spontaneous GnRH neuron firing rate is low at 3 weeks of age compared to controls but is increased in adulthood.[20,23] The developmental and PNA-induced changes in spontaneous GnRH neuron activity could be the result of altered neurotransmission to these cells and/or changes in their intrinsic properties. PNA treatment increases the frequency of GABAergic neurotransmission to GnRH neurons in 3-week-old and adult females.[17,24] Unlike most neurons, GnRH neurons maintain higher intracellular chloride concentration and activation of $GABA_A$ receptors can thus excite these neurons.[26,27] Despite receiving more frequent GABAergic transmission, however, GnRH neuron activity in 3-week-old PNA females is lower than controls,[23] suggesting that GnRH neurons from PNA females at this age respond differently to GABAergic input. Supporting this postulate, local GABA application increased firing in only about 30% of GnRH neurons from 3-week-old PNA females compared to 100% of neurons from 3-week-old control females and control and PNA adults.[24] The reduced response to GABA in 3-week-old PNA females is not attributable to differences from 3-week-old control in the baseline membrane potential or intracellular chloride concentration.[24] Together these findings suggest changes intrinsic to GnRH neurons might regulate how they respond to synaptic input and thus contribute to the altered firing rate.

In this regard, GnRH neurons from control and PNA adults fire more action potentials than control and PNA females at 3 weeks of age in response to the same amount of current injection.[28] Further, in adulthood the afterhyperpolarization potential of the action potential is larger and delayed relative to prepubertal mice.[28] The ionic changes underlying these differences are unknown. Here, we focus on voltage-gated potassium currents, which play a major role in determining the response of neurons to the inputs they receive, in shaping firing rate and in the repolarization characteristics of neurons.[29–32] GnRH neurons display two primary voltage-gated potassium currents, a fast transient current and a residual, delayed-rectifier-like current.[33] We tested the hypotheses that their properties change with age and with PNA treatment.

2 | MATERIALS AND METHODS

All chemicals were acquired from Sigma-Aldrich (St. Louis, MO, USA) unless noted otherwise.

2.1 | Animals

GnRH-GFP (Tg(Gnrh1-EGFP)51 Sumo MGI:6158457) mice were bred in our colony.[34] All mice were provided with ad libitum water and Harlan 2916 (non-breeders) or 2919 (breeders) chow. Mice were held on a 14:10 light/dark cycle with lights on at 3AM Eastern Standard Time. To generate female PNA mice, female GnRH-GFP transgenic mice on a C57Bl/6J background and a CD1 female were bred with a C57Bl/6J male. The CD1 dam assists in providing maternal care and nutrition. Females were monitored daily for a copulatory plug (Day 1 of pregnancy). On Days 16–18 of pregnancy, GnRH-GFP dams were injected subcutaneously with 225 μg/day of dihydrotestosterone (DHT) in 50 μL sesame oil for PNA treatment or sesame oil for controls. Litter sizes were adjusted to 4–15 pups by culling the CD1 pups, identifiable by size and coat color, to standardize nutrition. Adult female mice were studied on the morning of diestrus, determined by vaginal cytology and confirmed by uterine mass. All procedures were approved by the Institutional Animal Care and Use Committee of the University of Michigan.

2.2 | Verification of PNA phenotype

Electrophysiological studies were done on 3-week-old (18–21 days, before VO) and adult (84–130 days) diestrous females. PNA-induced differences were confirmed for the prepubertal mice in littermates raised to adulthood, as the PNA phenotype is consistent among littermates. PNA status was measured by monitoring age at which VO occurred, estrous cyclicity via vaginal lavage for 14 consecutive days

and measuring anogenital distance (AGD) between 70 and 73 days of age (average of three successive daily measures).

2.3 | Brain slice preparation

All solutions were bubbled with 95% O_2/5% CO_2 for at least 15 min before use and throughout experimental recordings. Brain slices were prepared as described.[35] Brains were removed and placed in ice-cold sucrose saline containing the following (in mM): 250 sucrose, 3.5 KCl, 26 $NaHCO_3$, 10 D-glucose, 1.25 Na_2HPO_4, 1.2 $MgSO_4$, and 3.8 $MgCl_2$ (350 mOsm). Coronal slices (300 μm) through the preoptic and anterior hypothalamic region were cut with a Leica VT1200S Microtome (Leica Biosystems, Buffalo Grove, IL). Slices were incubated for 30 min at room temperature (~21–23°C) in 50% sucrose saline and 50% artificial cerebrospinal fluid (ACSF, containing [in mM]: 135 NaCl, 3.5 KCl, 26 $NaHCO_3$, 10 D-glucose, 1.25 Na_2HPO_4, 1.2 $MgSO_4$, 2.5 $CaCl_2$, 315 mOsm, pH 7.4). Slices were then transferred to 100% ACSF at room temperature for 0.5–5 h before recording. No changes in properties were associated with time from slice preparation to recording. A minimum of five mice from at least four litters were studied per group; up to three recordings were used per mouse.

2.4 | Recording solutions and data acquisition

Brain slices were transferred to a recording chamber continuously perfused with carboxygenated ACSF (3 mL/min) maintained at 30–31°C with an inline-heating unit (Warner Instruments Model SH-27B). Potassium currents were pharmacologically isolated by blocking fast sodium (2 μM tetrodotoxin; Tocris Bioscience or Abcam) and calcium (300 μM $NiCl_2$) channels as well as ionotropic receptors for GABA (100 μM picrotoxin) and glutamate (20 μM D-APV and 10 μM CNQX; Tocris Bioscience). The pipet solution contained (in mM): 120 K gluconate, 20 KCl, 10 HEPES, 5 EGTA, 0.1 $CaCl_2$, 4 MgATP, and 0.4 NaGTP (305 mOsm, 7.2 pH with NaOH). This solution was based on the native intracellular chloride concentrations in GnRH neurons that was determined using gramicidin perforated-patch recordings.[26] A 14.5 mV liquid junction potential was negated online before each recording. GFP-positive GnRH neurons were visualized with infrared differential interference contrast and fluorescence microscopy on an Olympus BX51WI microscope. Recordings were made using an EPC-10 patch-clamp amplifier and a computer running PatchMaster software (HEKA Elektronik). All current measurements were acquired at 20 kHz and filtered at 10 kHz. Recording quality and passive properties were monitored throughout experiments from the averaged membrane current response to 16 hyperpolarizing voltage steps from −70 mV (5 mV, 20 ms). Data were analyzed using WaveMetrics IgorPro (Sutter Instruments). Only recordings with an input resistance of >500 MΩ, stable compensated series resistance of <15 MΩ and a stable capacitance (8–20 pF) were used for analysis.

2.5 | Activation/inactivation of voltage-gated potassium currents

GnRH neurons display two major voltage-gated potassium currents, a fast transient (I_A-like) current and a slow residual (I_K-like) current. The distinct voltage dependence of inactivation of the transient and residual currents was used to isolate them. GnRH neurons were given a prepulse step to −100 mV or −40 mV for 500 ms. The −40 mV or −100 mV prepulse was followed by a family of voltage steps from −100 mV to +50 mV (500 ms) in 10 mV increments, and then a final step to −10 mV for 50 ms. Pilot studies showed that a 500 ms prepulse at −40 mV results in full inactivation of the transient component, leaving the residual current mostly unchanged, and the prepulse at −100 mV for 500 ms completely removes I_A inactivation, yielding total current. The transient current was mathematically isolated by subtracting the current with the −40 mV prepulse from that obtained with the −100 mV prepulse at each voltage step. Activation of the transient current was estimated using the peak current during the final test pulse to −10 mV that followed the family of voltage steps. Leak current was calculated from an average of 4 sweeps at 1/8 amplitude (modified P/−8) from a baseline potential of −70 mV[36] and subtracted online.

2.6 | Time dependence of inactivation and recovery following inactivation for transient current

To measure the time dependence of inactivation, a 500 ms prepulse at −100 mV was used to remove inactivation. Then, membrane potential was stepped to −40 mV for 1, 2, 4, 8, 16, 32, 64, 128, 256, 512, and 1024 ms, followed by a test pulse at −10 mV to measure the peak current. The non-inactivating component at −10 mV after the 1024 ms inactivation step was subtracted from all of the other traces to isolate the transient current. To measure the time dependence of recovery from inactivation of the transient current, membrane potential was held at −40 mV (500 ms) to fully inactivate the fast transient component. Then, membrane potential was stepped to −100 mV for 1, 2, 4, 8, 16, 32, 64, 129, 512, and 1024 ms, followed by a test pulse at −10 mV to measure the peak current. The non-inactivating component at 1 ms recovery was subtracted from each of the other traces to isolate the transient component.

2.7 | Data analysis

Current density was calculated by dividing the maximum current by the capacitance for each recording. The driving force was calculated using the Goldman–Hodgkin–Katz (GHK) equation[37,38]:

$$\mathrm{GHK}(V) = V\left(\frac{zF}{RT}\right)\left(e^{\frac{zF}{RT}(V-E_K)} - 1\right)/\left(e^{\frac{zF}{RT}V} - 1\right),$$

where V is the step potential and E_K was calculated to be −92.6 mV after activity corrections.[39] Potassium conductance was estimated by dividing peak current by driving force. Conductance values were used to plot the voltage-dependent activation of transient and sustained potassium current components.

These data were plotted as a function of voltage and fit with the Boltzmann equation:

$$I(V) = \frac{1}{1 + e^{-\frac{kF}{RT}(V - V_{0.5})}},$$

where V is the command membrane potential of the step, $V_{0.5}$ is the potential at which half the current was activated or inactivated, and k is the "slope factor," F is the Faraday constant, R is the gas constant, and T is the absolute temperature. For inactivation, the driving force is the same for all cells because it is measured at the same membrane potential (test pulse 0 mV); because of this, there is no need to convert to conductance for comparison. The Boltzmann equation was thus fit to the normalized peak current as a function of the inactivating prepulse (−100 mV to −30 mV). The Boltzmann fit was used to estimate the $V_{0.5}$ activation, $V_{0.5}$ inactivation, and the slope factors.

To characterize the time dependence of inactivation and recovery, the relevant current was normalized to the maximum peak current for each cell and plotted as a function of duration of the prepulse. This was fit to a double exponential equation to account for fast and slow components:

$$Y = Y_{\text{end}} + (Y_{\text{start}} - Y_{\text{end}}) \times \left(F_{\text{fast}} \times e^{(-K_{\text{fast}} \times \tau_{\text{fast}})}\right) + (1 - F_{\text{fast}}) \times e^{(-K_{\text{slow}} \times \tau_{\text{slow}})}.$$

In this equation, Y_{start} is the Y value when X (time; ms) is zero; this value is held constant either at 1 for time-dependence of inactivation or 0 for the time-dependence of recovery from inactivation. Y_{end} is the Y-value when X is 1024 ms; this is held constant at either 0 for the time-dependence of inactivation or 1 for the time-dependence of recovery from inactivation. F_{fast}, the percent of the fast component, was held constant at 90% for both time-dependence fits. K_{fast} and K_{slow} are the rate constants, expressed in the reciprocal of the X-axis time units. Values for the fast (τ_{fast}) and slow (τ_{slow}) time constants are reported.

2.8 | Statistics

Data were tested for normal distribution with the Shapiro–Wilk test. Data are reported as the mean ± SEM or median ± IQR, as appropriate, with the individual values shown when practical. Statistical tests were chosen based on experimental design and data distribution and are specified in the results. Statistical comparisons and all graphs were made in Prism 10.1.1 (GraphPad Software), except for the statistical analysis of the proportion of time spent in each estrous cycle phase, for which RStudio was used[40–42] as Prism is unable to run the appropriate chi-squared tests.[43,44] Analysis in R (R version 4.3.1 "Beagle Scouts") using RStudio (RStudio Team, 2023) and a combination of open-sourced packages including, rstatix[43] and flextable,[44] for which the "chisq_test," "chisq_descriptives," "row_wise_fishers_test," and the "p.adjust.method" function were used to run the chi-squared tests. Significance was set at $p < .05$.

3 | RESULTS

3.1 | Verification of prenatal androgenization phenotype

PNA-induced differences were confirmed in this study. Consistent with previous observations,[17,20,23,28,45] VO occurred at a younger age (Mann–Whitney U-test) and a lower body mass (Mann–Whitney U-test) in PNA ($n = 24$) than control ($n = 28$) females (Figure 1A,B; Table 1). AGD was increased in adult PNA females (two-tailed, unpaired Student's t-test; Figure 1C; Table 1) and estrous cycles were disrupted. Specifically, PNA females spent more time in diestrus and less time in proestrus and estrus than controls (χ^2; Figure 1D,E; Table 1).

3.2 | Recording quality parameters and passive properties of GnRH neurons

Passive properties and series resistance were used to assess the quality of electrophysiological recordings (Figure 2). There were no differences among these parameters among any of the recording protocols, and all recordings were thus combined for quality assessment (two-way ANOVA; Table 2). There were no differences in passive properties or series resistance among groups.

3.3 | Voltage-dependent properties of the transient potassium current change with development and PNA treatment

First, we characterized the amplitude, density, and voltage-dependences of activation and inactivation of the transient current (Figure 3; Table 3). Figure 3A shows representative traces. Neither development nor PNA treatment alter the maximum peak current measured in GnRH neurons at −10 mV (Figure 3B; two-way ANOVA/Fishers least significant difference [LSD]). There was, however, an interaction between development and PNA treatment on transient current density. This difference appears to be driven by a PNA-induced increase in this parameter at 3 weeks of age (Figure 3C; two-way ANOVA/Fisher's LSD). Figure 3D shows the normalized current inactivation (left) and normalized conductance activation (right) as a function of voltage for the transient current. The $V_{0.5}$ of activation and $V_{0.5}$ of inactivation were more

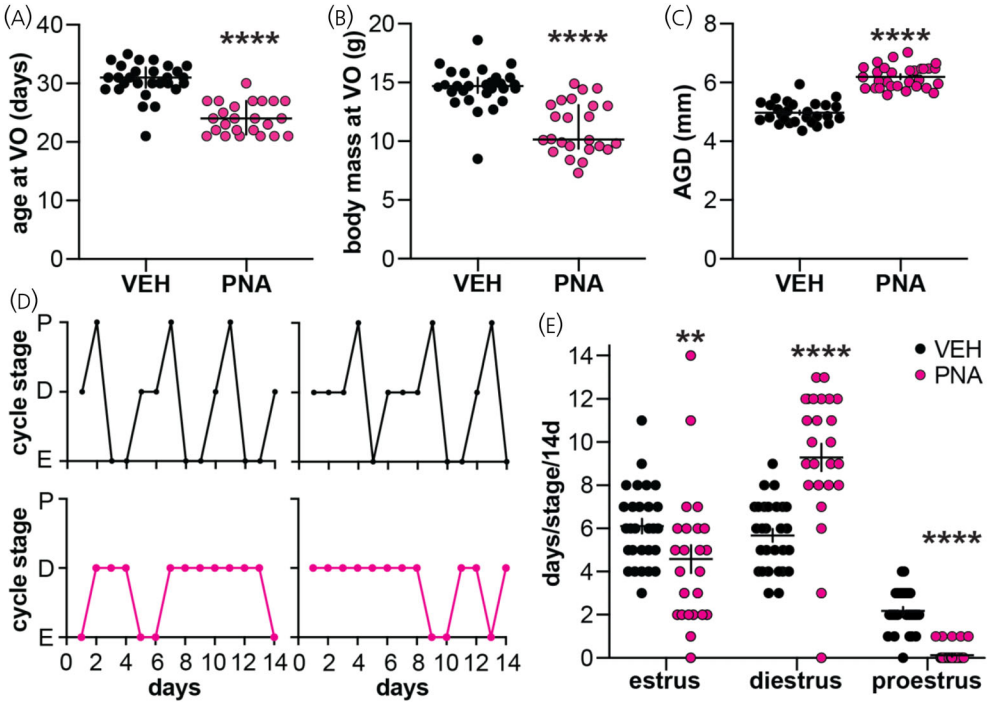


FIGURE 1 Confirmation of PNA phenotype. (A–C) Individual values and median + the interquartile range (IQR) for age at vaginal opening (VO; A) and body mass at VO (B). Individual values and mean ± SEM for anogenital distance in adulthood (AGD, C). (D) Representative estrous cycles over 14 days. P, proestrus; D, diestrus; E, estrus (top, vehicle; bottom, PNA). (E) Individual values and mean ± SEM for days in each cycle over 14 days. Statistical parameters are in Table 1. *$p < 0.05$, **$p < 0.005$, ***$p < 0.001$, ****$p < 0.0001$.

TABLE 1 Statistical parameters characterizing the PNA phenotype.

Property	VEH median and interquartile range (IQR)	PNA median and interquartile range (IQR)	Mann–Whitney *U* test	Two-tailed *p*-value
Age at vaginal opening (d)	31.0 (IQR 29.25–32.5)	24.0 (IQR 21.25–27.00)	$U = 43$	**$p < 0.0001$**
Body mass (g) at vaginal opening	14.7 (IQR 14.13–15.4)	10.15 (IQR 9.38–13.08)	$U = 71.50$	**$p < 0.0001$**

Property	Mean ± SEM for AGD	
AGD (mm)	**VEH**	**PNA**
	5.0 ± 0.07	6.2 ± 0.08

Unpaired, two-tailed Student's *t* test	Mean difference (VEH–PNA)	Effect size r^2
$t(10.98)$, df = 48; **$p < .0001$**	Diff [CI, 0.979, 1.418] 1.198 ± 0.11	$r^2 = .72$

	Mean ± SEM for days spent across estrous cycle state	
Cycle stage	**VEH**	**PNA**
Estrus	6.0 ± 0.4	4.6 ± 0.6
Diestrus	5.8 ± 0.3	9.3 ± 0.6
Proestrus	2.1 ± 0.2	0.1 ± 0.1

Property	χ^2 test		
Estrous cycle stage distribution	$\chi^2 = 66.194$, $n = 671$, df = 2, **$p < .0001$**		
	Estrus	**Diestrus**	**Proestrus**
Std. residual	2.736304	−6.388093	6.823246
Fisher's exact test; Bonferroni adjusted	**$p = 0.02$**	**$p < 0.0001$**	**$p < .0001$**

Note: Bold indicates $p < .05$.

depolarized in cells from 3-week-old than adult control mice (Figure 3E,F; two-way ANOVA/Fisher's LSD). PNA treatment hyperpolarized the $V_{0.5}$ of inactivation at 3 weeks of age. Neither development nor PNA treatment altered the slope factor of activation or inactivation of the transient current (Figure 3G,H; two-way ANOVA/Fisher's LSD).

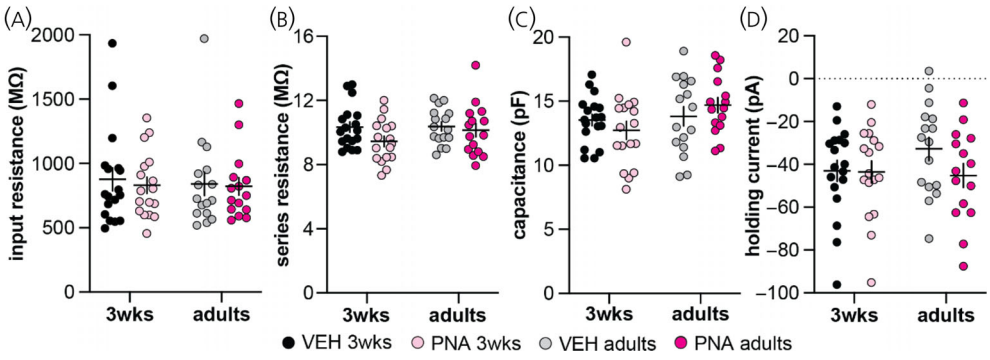


FIGURE 2 Recording quality and passive property parameters. (A–D) Individual values and mean ± SEM for input resistance (A), compensated series resistance (B), capacitance (C), and holding current (D). Numbers and statistical parameters are in Table 2.

TABLE 2 Descriptive statistics and statistical parameters from two-way ANOVA for recording quality parameters and passive properties.

Protocol	VEH 3 weeks	PNA 3 weeks	VEH adults	PNA adults
Voltage-dependence of activation & inactivation (transient & residual currents)	$n = 14$ cells from 7 mice from 5 litters	$n = 16$ cells from 10 mice from 7 litters	$n = 14$ cells from 7 mice from 6 litters	$n = 14$ cells from 10 mice from 10 litters
Time dependence of inactivation (transient current)	$n = 13$ from 8 mice from 4 litters	$n = 13$ cells from 8 mice from 7 litters	$n = 13$ cells from 7 mice from 6 litters	$n = 15$ cells from 10 mice from 10 litters
Time dependence of recovery following inactivation (transient current)	$n = 13$ cells from 8 mice from 4 litters	$n = 13$ cells from 8 mice from 5 litters	$n = 13$ cells from 8 mice from 7 litters	$n = 14$ cells from 9 mice from 9 litters
Descriptive statistics (mean ± SEM)				
Property	**VEH 3 weeks**	**PNA 3 weeks**	**VEH adults**	**PNA adults**
Series resistance (MΩ)	10.3 ± 0.3	9.4 ± 0.3	10.4 ± 0.3	10.1 ± 0.4
Input resistance (MΩ)	877.4 ± 89.2	830.0 ± 62.0	841.5 ± 89.9	821.9 ± 67.7
Capacitance (pF)	13.5 ± 0.4	12.7 ± 0.7	13.8 ± 0.7	14.7 ± 0.6
Holding current (pA)	−43.0 ± 4.9	−43.6 ± 5.1	−32.8 ± 5.3	−45.236 ± 5.546
Two-way ANOVA				
Property	**Age**	**Treatment**	**Interaction**	
Series resistance (MΩ)	Diff, −0.3643 [CI, −1.541, 0.2098] $F(1,62) = 1.176$; $p = .2824$	Diff, 0.5641 [CI, −0.1040, 1.232] $F(1,62) = 2.848$; $p = .0965$	Diff, 0.6590 [CI, −0.6774, 1.995] $F(1,62) = 0.9716$; $p = .3281$	
Input resistance (MΩ)	Diff, 22.03 [CI, −136.2, 180.3] $F(1,62) = 0.08615$; $p = 0.7749$	Diff, 34.47 [CI, −124.8, 191.7] $F(1,62) = 0.1788$; $p = 0.6739$	Diff, 27.80 [CI, −288.7, 344.3] $F(1,62) = 0.03083$; $p = 0.8612$	
Capacitance (pF)	Diff, −1.129 [CI, −2.380, 0.1214] $F(1,62) = 3.258$; $p = 0.0759$	Diff, −0.03315 [CI, −1.284, 1.217] $F(1,62) = 0.002808$; $p = 0.9579$	Diff, 1.690 [CI, −0.8115, 4.191] $F(1,62) = 1.824$; $p = 0.1818$	
Holding current (pA)	Diff, −4.307 [CI, −14.78, 6.163] $F(1,62) = 0.6762$; $p = 0.4141$	Diff, 6.483 [CI, −3.986, 16.95] $F(1,62) = 1.532$; $p = 0.2204$	Diff, −11.96 [CI, −32.90, 8.890] $F(1,62) = 1.303$; $p = 0.2580$	

3.4 | Time-dependence of inactivation and recovery from inactivation of the transient potassium current change with development and PNA treatment

Next, we characterized the time-dependence of inactivation (Figure 4A–D) and recovery from inactivation (Figure 4E–H) of the transient current (Table 4). Representative traces are in Figure 4A,E, and the time-dependence of inactivation and removal of inactivation in Figure 4B,F. Neither age nor PNA treatment altered the fast time constant of inactivation (Figure 4C,D). In contrast, there was an increase in the fast time constant for recovery in PNA adults compared to both 3-week-old PNA mice and adult controls (Figure 4G,H; two-way ANOVA/Fisher's LSD). Neither the slow time constant for inactivation nor recovery were affected by any treatment.

3.5 | Development and PNA treatment interact to alter the voltage-dependence of activation of the residual current

We next tested if development and/or PNA treatment alter the residual current (Figure 5A). Neither maximum peak current nor current density was altered by development or PNA treatment alone (Figure 5B,C; two-way ANOVA; Table 5). Figure 5D shows the

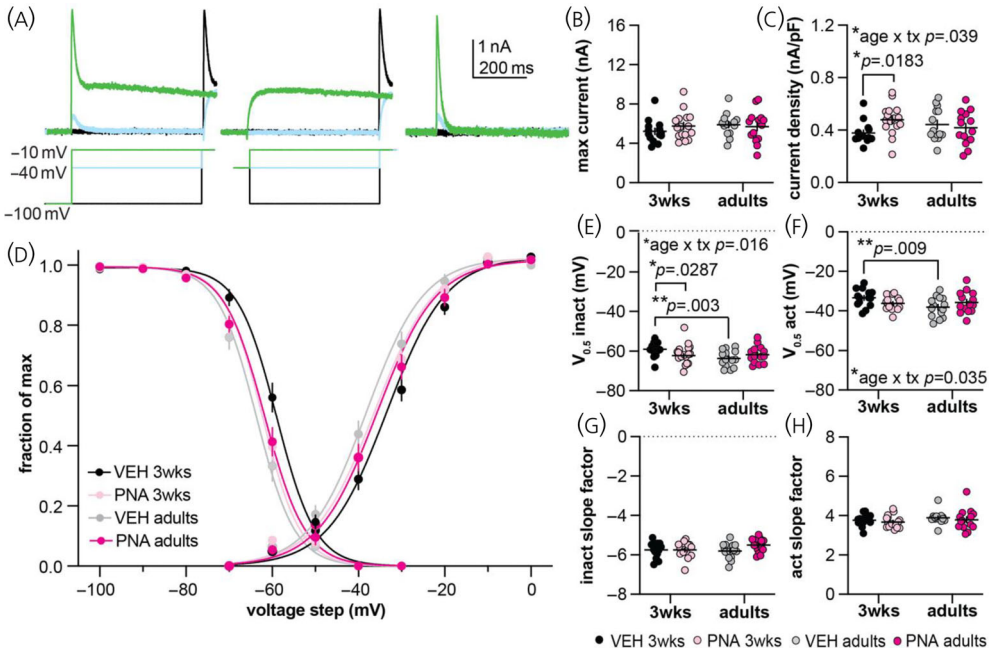


FIGURE 3 Characterization of the transient potassium current. (A) Representative traces illustrating mathematical isolation of the transient current (right) by subtracting the −40 mV prepulse traces in the middle panel from the −100 mV prepulse traces in the left panel. Only three voltage-steps are shown for clarity. (B, C) Individual values and mean ± SEM for maximum current (B) and current density (C). (D) Voltage-dependence of inactivation (left) and activation (right). Fraction of maximum refers to normalized current for inactivation and normalized conductance for activation. Boltzmann fits of the mean data are shown for each group. (E–H) Individual values and mean ± SEM $V_{0.5}$ activation ($V_{0.5}$ act, E), $V_{0.5}$ inactivation ($V_{0.5}$ inact, F), inactivation slope factor (G), and activation slope factor (H). For (B, C, and E–H), two-way ANOVA/Fisher's LSD; statistical parameters are in Table 3; tx, treatment. Error bars are often within the size of the symbol.

normalized conductance as a function of voltage estimated from the residual current. There was an age by treatment interaction on the $V_{0.5}$ of activation. This was attributable to a development-related hyperpolarization of $V_{0.5}$ activation in control mice and a PNA-induced depolarization of $V_{0.5}$ activation in adult mice (Figure 5E). Neither development nor PNA treatment altered the slope factor of activation of the residual current (Figure 5F; two-way ANOVA).

4 | DISCUSSION

The pattern of GnRH/LH release can change in ways that promote reproduction, such as through the pubertal transition, and in ways that impair reproduction, such as persistent high-frequency release in women with PCOS. Changes in GnRH neuron firing rate are likely to underlie changes in GnRH release,[46] and potassium currents play a major role in sculpting neuronal firing activity.[29–32] Here, we demonstrate that changes in voltage-dependent potassium currents of GnRH neurons occur during pubertal development and that PNA treatment further alter some characteristics of these currents.

GnRH neurons express a fast transient potassium current[33,35] that responds to subthreshold changes in voltage and plays a role in regulating neuronal excitability and firing properties.[47] Transient current density was increased in GnRH neurons from PNA mice at 3 weeks of age compared to 3-week-old controls. This finding extends prior work in this PNA model that showed that GnRH neurons from PNA females have a lower spontaneous firing rate than controls at 3 weeks of age by providing a possible mechanistic explanation; greater transient potassium current density typically resists depolarization,[48] which may lead to cells initiating firing bouts less frequently in the absence of other changes. Further, the increased transient current density in 3-week-old PNA females could contribute to the blunted firing response to exogenous GABA exposure observed in GnRH neurons from PNA mice compared to controls at 3 weeks of age. Of interest, the increased transient current density in 3-week-old PNA females may be a compensatory mechanism initiated in GnRH neurons by the increased excitatory GABAergic neurotransmission at this age as a way of providing neuroprotection in PNA mice.[49–52]

In addition to current density, the voltage and time dependence of transient potassium currents help sculpt firing in excitable cells. Regarding the former, a clear development-associated hyperpolarization of both the inactivation and activation of the transient current occur in control mice. Hyperpolarization of inactivation in adults would tend to make less current available in the subthreshold range, perhaps contributing to increased excitability of adult GnRH neurons compared to those from prepubertal mice.[28] The hyperpolarization of activation in adult controls may sculpt aspects of the action potential spike, including the increased afterhyperpolarization potential.[28] In PNA females, there were no changes in either voltage-dependence of inactivation or activation with development. In contrast to the effects

TABLE 3 Descriptive statistics and statistical parameters from two-way ANOVA/Fisher's LSD for the voltage-dependent properties of the transient current.

Descriptive statistics (mean ± SEM)				
Property	**VEH 3 weeks**	**PNA 3 weeks**	**VEH adults**	**PNA adults**
$V_{0.5}$ activation (mV)	−33.4 ± 1.2	−36.3 ± 0.8	−38.2 ± 1.4	−35.7 ± 1.5
Activation slope factor	3.8 ± 0.3	3.7 ± 0.3	3.9 ± 0.3	3.8 ± 0.5
$V_{0.5}$ inactivation (mV)	−59.0 ± 0.005	−62.3 ± 0.9	−63.671 ± 1.1	−61.736 ± 1.2
Inactivation slope factor	−5.750 ± 0.103	−5.750 ± 0.095	−5.804 ± 0.106	−5.504 ± 0.095
Maximum current (pA)	5.2 ± 0.3	5.8 ± 0.3	5.9 ± 0.3	5.7 ± 0.43
Maximum current density (pA/pF)	0.38 ± 0.02	0.48 ± 0.0	0.44 ± 0.03	0.41 ± 0.034

Two-way ANOVA					
Property	**Age**	**Treatment**		**Interaction**	
$V_{0.5}$ activation (mV)	Diff, 2.108 [CI, −0.3297, 4.564]	Diff, 0.2094 [CI, −2.228, 2.647]		Diff, 5.265 [CI, 0.3891, 10.14]	
	$F(1,54) = 3.006$; $p = .0887$	$F(1,54) = 0.029965$; $p = .8638$		$F(1,54) = 4.687$; $\mathbf{p = .0348}$	
	Fisher's LSD	3-week VEH vs. 3-week PNA	3-week VEH vs. adult VEH	3-week PNA vs. adult PNA	Adult VEH vs. adult PNA
		$p = .0988$	$\mathbf{p = 0.0089}$	$p = 0.7578$	$p = .1712$
Activation slope factor	Diff, −0.1189 [CI, −0.3199, 0.08204]	Diff, 0.09526 [CI, −0.1057, 0.2962]		Diff, −0.007502 [CI, −0.3944, 0.4094]	
	$F(1,54) = 1.408$; $p = .2406$	$F(1,54) = 0.9030$, $p = .3462$		$F(1,54) = 0.0014$, $p = .9703$	
$V_{0.5}$ inactivation (mV)	Diff, 2.081 [CI, −0.0300, 4.192]	Diff, 0.6790 [CI, −1432, 2.790]		Diff, 5.228 [CI, 1.005, 9.450]	
	$F(1,54) = 3.906$; $p = .0532$	$F(1,54) = 0.4158$; $p = 0.5218$		$F(1,43) = 6.162$; $\mathbf{p = .0162}$	
	Fisher's LSD	3-week VEH vs. 3-week PNA	3-week VEH vs. adult VEH	3-week PNA vs. adult PNA	Adult VEH vs. adult PNA
		$\mathbf{p = .0287}$	$\mathbf{p = 0.0030}$	$p = .7175$	$p = 0.2064$
Inactivation slope factor	Diff, −0.09627 [CI, −0.2965, 0.1040]	Diff, −0.1496 [CI, −0.3498, 0.05064]		Diff, 0.2993 [CI, −0.1011, 0.6998]	
	$F(1,54) = 0.9292$, $p = .3394$	$F(1,54) = 2.243$, $p = .1400$		$F(1,54) = 2.246$, $p = 0.1398$	
Maximum current (pA)	Diff, −0.3096 [CI, −01.020, 0.4009]	Diff, −0.1793 [CI, −0.8898, 0.5312]		Diff, −0.7400 [CI, −2.161, 0.6810]	
	$F(1,54) = 0.7634$, $p = 0.3861$	$F(1,53) = 0.2559$, $p = 0.6150$		$F(1,54) = 1.0909$, $p = 0.3011$	
Maximum current density (pA/pF)	Diff, 0–0.0018 [CI, −0.06185, 0.05832]	Diff, −0.03836 [CI, −0.09844, 0.02172]		Diff, −0.1283 [CI, −0.2464, −0.0061]	
	$F(1,54) = 0.0035$, $p = 0.9532$	$F(1,54) = 1.6838$, $p = 0.2060$		$F(1,54) = 4.439$, $\mathbf{p = 0.0398}$	
	Fisher's LSD	3-week VEH vs. 3-week PNA	3-week VEH vs. adult VEH	3-week PNA vs. adult PNA	Adult VEH vs. adult PNA
		$\mathbf{p = 0.0183}$	$p = 0.1376$	$p = 0.1468$	$p = 0.5674$

Note: Bold indicates $p < .05$.

of development on voltage dependence of inactivation, PNA treatment had a more marked effect on its time dependence. Most notably, recovery from inactivation took longer in PNA adults in comparison to other groups. This may be a contributing factor to the increased spontaneous activity observed in GnRH neurons from PNA mice in adulthood.[23] Together these data indicate changes in transient current properties occur concomitant with pubertal development, and that prenatal androgen exposure both disrupts typical developmental changes in this current and induces an independent shift in properties.

The speculative attribution of the effects of specific properties of the transient current to prior observations in GnRH neuron physiology in these same animal models is done with caution for several reasons. First, different properties of the same macroscopic current can have different predicted effects on neuronal output in the same animal model. For example, changes in voltage-dependence of inactivation of the transient current from 3 weeks of age to adults in control mice might increase excitability, whereas the lack of difference in transient current density between these same groups might predict no change.

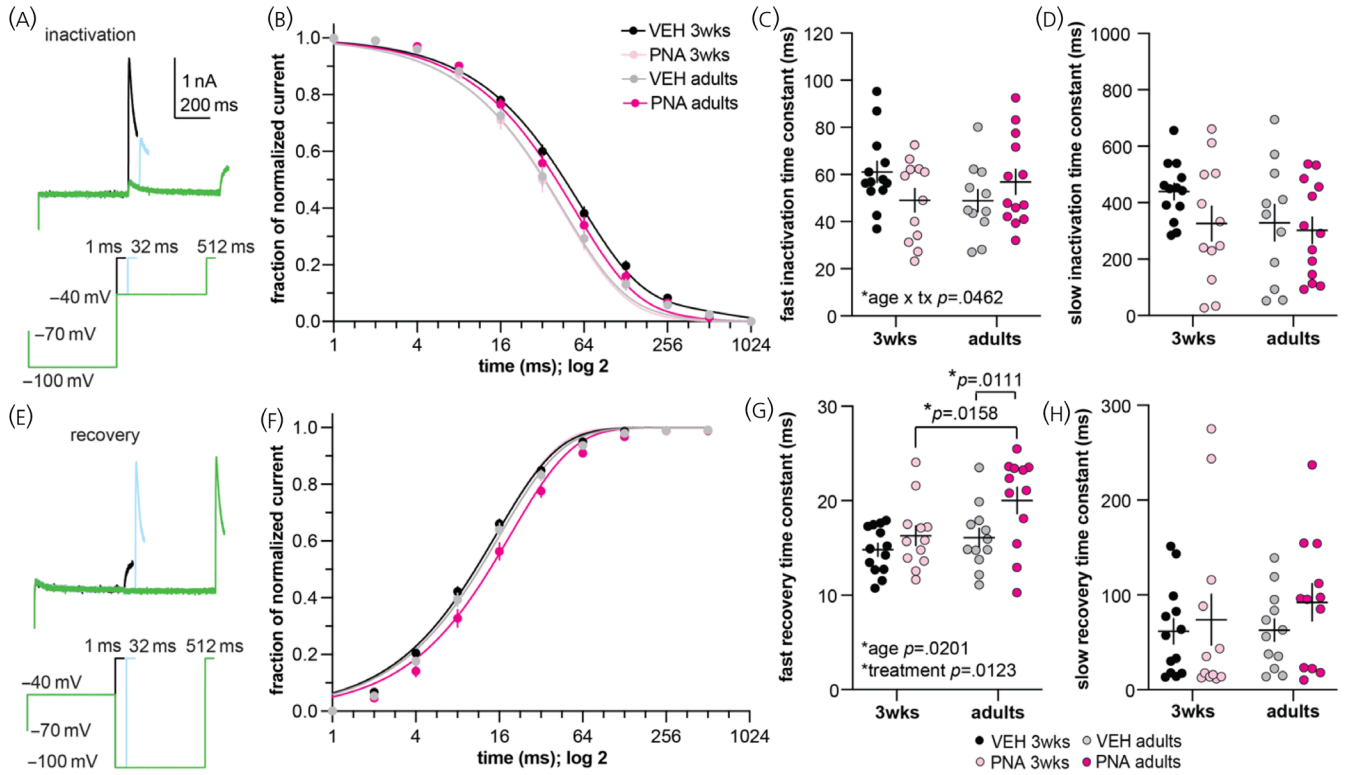


FIGURE 4 Characterization of the time dependence of inactivation and recovery from inactivation of the transient current in GnRH neurons. (A, E) Representative traces illustrating the time dependence of transient current inactivation (A) and recovery from inactivation (E). Only three voltage-steps are shown for clarity (bottom). (B, F) Current was normalized to the maximum and plotted as a function of time (B, inactivation; F, recovery). The solid lines represent the double exponential equation evaluated using the mean fast and slow time constants for each group. (C, D, G, H) Individual values and mean ± SEM for the fast time constant of inactivation (inact; C), the slow time constant of inactivation (inact; D), the fast time constant of recovery (recov; G), and the slow time constant of recovery (recov; H). (C, D, G, H) Two-way ANOVA/Fisher's LSD; statistical parameters are in Table 4.

Second, the direction of change induced by a particular property in isolation is a postulate. For example, increased transient current can be associated with reduced excitability[35] but can also induce membrane potential changes that enhance recovery from inactivation of the fast sodium current and thus increase firing rate.[53] Third, the effects of the transient potassium current on firing and excitability do not occur in isolation but are integrated with changes in other GnRH neuron intrinsic properties that may occur as the animal goes through puberty and/or in response to PNA treatment. In this regard, we observed age-dependent changes in the activation of the residual potassium current in controls but PNA treatment-dependent shifts in this property in adults. Activation of this current typically occurs at the depolarized membrane potentials achieved during an action potential. The residual current is important in repolarizing the membrane, sculpting action potential shape[54,55] and determining the generation of subsequent action potentials in a burst.[54] In adult control females, hyperpolarized residual current activation might contribute to reduced spontaneous firing activity of GnRH neurons in the group compared to 3-week-old controls and to adult PNA females. Fourth, there are documented changes in GABAergic fast synaptic input with age and PNA treatment that will also contribute to determining the overall firing rate of these cells.[17,24] Finally, other factors, such as neuromodulator input, may also differ among groups. Of interest in this regard, no difference was observed in the spontaneous firing rate of arcuate kisspeptin neurons among these same four groups,[56] but interactions with other neuromodulatory neurons and with non-neuronal cells could alter GnRH neuron output in a PNA-treatment and/or age-dependent manner. Computational modeling would be one way to address these interactions, but there are no data on the other intrinsic properties of GnRH neurons in these animal models, limiting the utility of this approach at present.

The observed changes in the voltage- and time-dependent properties of potassium currents in this study extend work in other brain regions indicating these currents change across development. For example, in acutely dissociated large aspiny neurons, transient current inactivation is depolarized and occurs faster with increasing age; this may contribute to reduced spike latency in mature versus young neurons.[57] Developmental changes in voltage-dependent potassium currents are associated with establishing reliable spiking in the calyx of Held.[58] Potassium current alterations can also underlie neuropathological conditions, including pain,[59] neurodegeneration,[60] and epilepsy.[61] Within the reproductive neuroendocrine system, changes in potassium currents, in particular the transient current, are associated with changes in GnRH and arcuate kisspeptin neuron physiology. In a

TABLE 4 Descriptive statistics and statistical parameters from two-way ANOVA/Fisher's LSD for the time-dependence of inactivation and recovery from inactivation for the transient current.

Descriptive statistics (mean ± SEM)				
Property	**VEH 3 weeks**	**PNA 3 weeks**	**VEH adults**	**PNA adults**
Fast inactivation time constant (ms)	61.1 ± 4.4	54.4 ± 5.6	48.9 ± 4.7	56.9 ± 5.3
Slow inactivation time constant (ms)	439.7 ± 29.1	325.9 ± 61.4	329.1 ± 64.9	301.9 ± 46.7
Fast recovery time constant (ms)	14.8 ± 0.7	16.3 ± 1.0	16.1 ± 1.0	20.0 ± 1.4
Slow recovery time constant (ms)	61.6 ± 13.2	73.8 ± 26.8	62.8 ± 11.8	92.2± 19.7

Two-way ANOVA					
Property	**Age**	**Treatment**		**Interaction**	
Fast inactivation time constant (ms)	Diff, 2.185 [CI, −7.626, 12.00]	Diff, 1.992 [CI, −7.819, 11.80]		Diff, 19.97 [CI, 0.3468, 39.59]	
	$F(1,45) = 0.2102$; $p = 0.6559$	$F(1,45) = 0.1672$; $p = 0.6845$		$F(1,45) = 4.201$; $\mathbf{p = 0.0462}$	
	Fisher's LSD	3-week VEH vs. 3-week PNA	3-week VEH vs. VEH adult	3-week PNA vs. PNA adult	VEH adult vs. PNA adult
		$p = 0.0854$	$p = 0.0876$	$p = 0.2581$	$p = 0.2574$
Slow inactivation time constant (ms)	Diff, 67.35 [CI, −35.48, 173.5]	Diff, 70.51 [CI, −32.49, 173.5]		Diff, 86.51 [CI, −119.5292.5]	
	$F(1,45) = 1.734$; $p = 0.1945$	$F(1,45) = 1.901$; $p = 0.1748$		$F(1,45) = 0.7155$; $p = 0.4021$	
Fast recovery time constant (ms)	Diff, −2.507 [CI, −4.602, −0.4113]	Diff, −2.714 [CI, −4.810, −0.6188]		Diff, 2.443 [CI, −1.748, 6.634]	
	$F(1,45) = 5.805$; $\mathbf{p = 0.0201}$	$F(1,45) = 6.806$; $\mathbf{p = 0.0123}$		$F(1,45) = 1.379$; $p = 0.2465$	
	Fisher's LSD	3-week VEH vs. 3-week PNA	3-week VEH vs. VEH adult	3-week PNA vs. PNA adult	VEH adult vs. PNA adult
		$p = 0.3110$	$p = 0.3824$	$\mathbf{p = 0.0158}$	$\mathbf{p = 0.0111}$
Slow recovery time constant (ms)	Diff, −9.799 [CI, −47.37, 27.77]	Diff, −20.79 [CI, −58.36, 16.78]		Diff, 17.10 [CI, −58.04, 92.24]	
	$F(1,45) = 0.2760$; $p = 0.6019$	$F(1,45) = 1.242$; $p = 0.2709$		$F(1,45) = 0.2100$; $p = 0.6490$	

Note: Bold indicates $p < .05$.

model for estradiol positive feedback in which GnRH neurons are more active and more excitable,[62,63] transient current density is suppressed and other properties shifted in comparison to a gonadectomized open feedback loop condition.[35] In contrast, no differences were found between the open loop and a model of negative feedback; there were also no differences in excitability between these groups.[33] Estradiol also reduces transient current amplitude in arcuate kisspeptin neurons; in these cells, reducing this current enhances synaptic response and is associated with altered firing activity.[64] Of note, most prior studies on GnRH and kisspeptin neuron currents were done in adults, thus no developmental data are available. The steroid regulation of these currents is nonetheless applicable to the present work. The increased production of sex steroids that occurs with puberty might be the catalyst behind the developmental change observed in potassium currents observed in cells from control mice, as well as excitability and the GnRH neuron transcriptome.[28,45] Steroidogenesis is also altered in adult PNA mice, which have increased testosterone levels.[17,21,65] While many studies have examined estrogen effects on potassium currents in neuronal populations,[33,35,55,64,66] we found no studies of androgen effects on central neurons. Work in the cardiovascular system suggests androgen-associated changes in potassium currents. Cardiovascular disease, including arrhythmias, are more common in men.[67] Electrocardiogram QTc intervals are similar among prepubertal males and female and adult females, whereas adult males have shorter QTc intervals.[68–70] In rat cardiomyocytes, dihydrotestosterone (DHT), a non-aromatizable androgen, upregulates the delayed-rectified potassium channel and shortens the electrocardiogram QT interval, which correspond to the action potential duration in ventricular cardiomyocytes, compared to castrated males without DHT treatment.[71] In immortalized pituitary GH3 cells, androgens rapidly and reversibly block a sustained current,[72] and in cancer cells, voltage-gated potassium currents are associated with cell proliferation.[73] These studies support the postulate that age and PNA-induced changes in sex steroid milieu in the present studies could be the

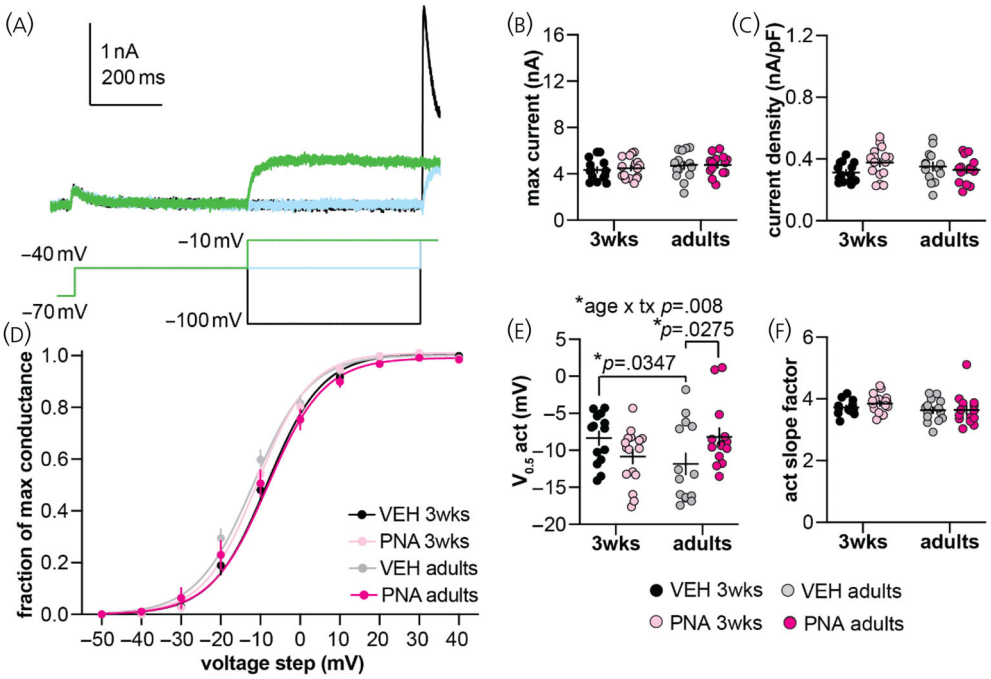


FIGURE 5 Characterization of the residual potassium current in GnRH neurons. (A) Representative traces illustrating the activation of the residual current (top). Only three voltage-steps are shown for clarity (bottom). B, C, Individual values and mean ± SEM for maximum current at −10 mV (B) and current density (C). (D) Voltage-dependence of activation plotted as fraction of maximum conductance; lines are Boltzmann fits of the mean data for each group. E, F, Individual values and mean ± SEM for $V_{0.5}$ activation ($V_{0.5}$ act, E), and activation (act) slope factor (F). (B, C, E, F) Two-way ANOVA/Fisher's LSD. Statistical parameters are in Table 5.

TABLE 5 Descriptive statistics and statistical parameters from two-way ANOVA/Fisher's LSD for the voltage-gated properties of the residual current.

Descriptive statistics (mean ± SEM)				
Property	**VEH 3 weeks**	**PNA 3 weeks**	**VEH adults**	**PNA adults**
$V_{0.5}$ activation (mV)	−8.4 ± 0.9	−10.8 ± 0.9	−11.8 ± 1.4	−8.2 ± 1.2
Activation slope factor	3.7 ± 0.1	3.8 ± 0.1	3.6 ± 0.1	3.6 ± 0.1
Maximum current (pA)	4.3 ± 0.2	4.5 ± 0.2	4.7 ± 0.3	4.8 ± 0.2
Maximum current density (pA/pF)	0.3 ± 0.02	0.4 ± 0.02	0.4 ± 0.03	0.3 ± 0.02

Two-way ANOVA				
Property	**Age**	**Treatment**		**Interaction**
$V_{0.5}$ activation (mV)	Diff, 0.4182 [CI, −1.826, 2.663]	Diff, −0.5773 [CI, −2.882, 1.667]		Diff, 6.135 [CI, 1.646, 10.62]
	$F(1,54) = 1396$, $p = .702$	$F(1,54) = 0.2660$, $p = 0.6082$		$F(1,54) = 7.508$, $\mathbf{p = 0.0083}$
	Fisher's LSD	3-week VEH vs. 3-week PNA	3-week VEH vs. adult VEH	3-week PNA vs. adult PNA / Adult VEH vs. adult PNA
		$p = 0.1157$	$\mathbf{p = 0.0347}$	$p = 0.0947$ / $\mathbf{p = 0.0275}$
Activation slope factor	Diff, 0.1510 [CI, −0.04228, 0.3444]	Diff, −0.06698 [CI, −0.2603, 0.1264]		Diff, −0.1181 [CI, −0.5047, 0.2686]
	$F(1,54) = 2.454$, $p = 0.1231$	$F(1,54) = 0.4824$, $p = 0.4903$		$F(1,54) = 0.3749$, $p = 0.5429$
Maximum current (pA)	Diff, −0.3357 [CI, −0.8520, 0.1806]	Diff, −0.09675 [CI, −0.6131, 0.4195]		Diff, −0.1177 [CI, −1.150, 0.9149]
	$F(1,54) = 01.700$, $p = 0.1979$	$F(1,54) = 0.1412$, $p = 0.7086$		$F(1,54) = 0.05218$, $p = 0.8202$
Maximum current density (pA/pF)	Diff, 0.004584 [CI, −0.04177, 0.05094]	Diff, −0.02063 [CI, −0.06698, 0.02573]		Diff, −0.08477 [CI, −0.1775, 0.0079939]
	$F(1,54) = 0.0393$, $p = 0.8436$	$F(1,54) = 7961$, $p = 0.3762$		$F(1,54) = 3.361$, $p = 0.0723$

Note: Bold indicates $p < .05$.

catalysts underlying changes observed in voltage-gated potassium currents.

The changes in voltage-dependent potassium currents in GnRH neurons described in this study likely play a role in shaping the activity of GnRH neurons through typical pubertal development and the changes induced by prenatal androgen exposure. Untangling these underlying mechanisms has implications for increased GnRH/LH release frequency and altered pubertal progression in hyperandrogenemic adolescents and individuals with PCOS.

AUTHOR CONTRIBUTIONS

Jennifer Jaime: Conceptualization; data curation; formal analysis; funding acquisition; investigation; methodology; visualization; writing – original draft; writing – review and editing. **R. Anthony DeFazio:** Conceptualization; formal analysis; writing – review and editing. **Suzanne M. Moenter:** Conceptualization; funding acquisition; methodology; project administration; resources; supervision; writing – original draft; writing – review and editing.

ACKNOWLEDGMENTS

We thank Laura Burger, J. Rudolph Starrett, and Elizabeth Wagenmaker for expert technical assistance, and Laura Burger, Xi Chen, Amanda Gibson, J. Rudolph Starrett, and Elizabeth Wagenmaker for editorial comments.

FUNDING INFORMATION

This work was supported by National Institute of Health (NIH)/Eunice Kennedy Shriver National Institute of Child Health and Human Development Grant R01HD104345 (to Suzanne M. Moenter). Support for Jennifer Jaime was provided by NIH T32HD079342 and F31HD110279.

CONFLICT OF INTEREST STATEMENT

The authors declare no competing financial interests.

PEER REVIEW

The peer review history for this article is available at https://www.webofscience.com/api/gateway/wos/peer-review/10.1111/jne.13373.

DATA AVAILABILITY STATEMENT

The data that support the findings of this study are available from the corresponding author upon reasonable request.

ORCID

Jennifer Jaime https://orcid.org/0000-0003-0870-2149
Suzanne M. Moenter https://orcid.org/0000-0001-9812-0497

REFERENCES

1. Clarke IJ, Cummins JT. The temporal relationship between gonadotropin releasing hormone (GnRH) and luteinizing hormone (LH) secretion in ovariectomized ewes. *Endocrinology*. 1982;111:1737-1739. doi:10.1210/endo-111-5-1737
2. Moenter SM, Brand RM, Midgley AR, Karsch FJ. Dynamics of gonadotropin-releasing hormone release during a pulse. *Endocrinology*. 1992;130:503-510. doi:10.1210/endo.130.1.1727719
3. Wildt L, Häusler A, Marshall G, et al. Frequency and amplitude of gonadotropin-releasing hormone stimulation and gonadotropin secretion in the rhesus monkey. *Endocrinology*. 1981;109:376-385. doi:10.1210/endo-109-2-376
4. Haisenleder DJ, Dalkin AC, Ortolano GA, Marshall JC, Shupnik MA. A pulsatile gonadotropin-releasing hormone stimulus is required to increase transcription of the gonadotropin subunit genes: evidence for differential regulation of transcription by pulse frequency in vivo. *Endocrinology*. 1991;128:509-517. doi:10.1210/endo-128-1-509
5. Legro RS. Diagnostic criteria in polycystic ovary syndrome. *Semin Reprod Med*. 2003;21:267-275. doi:10.1055/s-2003-43304
6. Tsutsumi R, Webster NJ. GnRH pulsatility, the pituitary response and reproductive dysfunction. *Endocr J*. 2009;56:729-737. doi:10.1507/endocrj.k09e-185
7. Sidhoum VF, Chan YM, Lippincott MF, et al. Reversal and relapse of hypogonadotropic hypogonadism: resilience and fragility of the reproductive neuroendocrine system. *J Clin Endocrinol Metab*. 2014;99:861-870. doi:10.1210/jc.2013-2809
8. Burt Solorzano CM, Beller JP, Abshire MY, Collins JS, McCartney CR, Marshall JC. Neuroendocrine dysfunction in polycystic ovary syndrome. *Steroids*. 2012;77:332-337. doi:10.1016/j.steroids.2011.12.007
9. McCartney CR, Campbell RE, Marshall JC, Moenter SM. The role of gonadotropin-releasing hormone neurons in polycystic ovary syndrome. *J Neuroendocrinol*. 2022;34:e13093. doi:10.1111/jne.13093
10. Yen SS, Vela P, Rankin J. Inappropriate secretion of follicle-stimulating hormone and luteinizing hormone in polycystic ovarian disease. *J Clin Endocrinol Metab*. 1970;30:435-442. doi:10.1210/jcem-30-4-435
11. Kazer RR, Kessel B, Yen SS. Circulating luteinizing hormone pulse frequency in women with polycystic ovary syndrome. *J Clin Endocrinol Metab*. 1987;65:233-236. doi:10.1210/jcem-65-2-233
12. Broekmans FJ, Fauser BC. Diagnostic criteria for polycystic ovarian syndrome. *Endocrine*. 2006;30:3-11. doi:10.1385/ENDO:30:1:3
13. Apter D, Bützow T, Laughlin GA, Yen SS. Accelerated 24-hour luteinizing hormone pulsatile activity in adolescent girls with ovarian hyperandrogenism: relevance to the developmental phase of polycystic ovarian syndrome. *J Clin Endocrinol Metab*. 1994;79:119-125. doi:10.1210/jcem.79.1.8027216
14. Yoo RY, Dewan A, Basu R, Newfield R, Gottschalk M, Chang RJ. Increased luteinizing hormone pulse frequency in obese oligomenorrheic girls with no evidence of hyperandrogenism. *Fertil Steril*. 2006;85:1049-1056. doi:10.1016/j.fertnstert.2005.09.037
15. Barber TM, Franks S. Genetics of polycystic ovary syndrome. *Front Horm Res*. 2013;40:28-39. doi:10.1159/000341682
16. Dapas M, Lin FTJ, Nadkarni GN, et al. Distinct subtypes of polycystic ovary syndrome with novel genetic associations: an unsupervised, phenotypic clustering analysis. *PLoS Med*. 2020;17:e1003132. doi:10.1371/journal.pmed.1003132
17. Sullivan SD, Moenter SM. Prenatal androgens alter GABAergic drive to gonadotropin-releasing hormone neurons: implications for a common fertility disorder. *Proc Natl Acad Sci U S A*. 2004;101:7129-7134. doi:10.1073/pnas.0308058101
18. Foecking EM, Szabo M, Schwartz NB, Levine JE. Neuroendocrine consequences of prenatal androgen exposure in the female rat: absence of luteinizing hormone surges, suppression of progesterone receptor gene expression, and acceleration of the gonadotropin-releasing hormone pulse generator. *Biol Reprod*. 2005;72:1475-1483. doi:10.1095/biolreprod.105.039800
19. Mahoney MM, Padmanabhan V. Developmental programming: impact of fetal exposure to endocrine-disrupting chemicals on gonadotropin-releasing hormone and estrogen receptor mRNA in

sheep hypothalamus. *Toxicol Appl Pharmacol*. 2010;247:98-104. doi:10.1016/j.taap.2010.05.017
20. Roland AV, Moenter SM. Prenatal androgenization of female mice programs an increase in firing activity of gonadotropin-releasing hormone (GnRH) neurons that is reversed by metformin treatment in adulthood. *Endocrinology*. 2011;152:618-628. doi:10.1210/en.2010-0823
21. Witham EA, Meadows JD, Shojaei S, Kauffman AS, Mellon PL. Prenatal exposure to low levels of androgen accelerates female puberty onset and reproductive senescence in mice. *Endocrinology*. 2012;153:4522-4532. doi:10.1210/en.2012-1283
22. Moore AM, Prescott M, Marshall CJ, Yip SH, Campbell RE. Enhancement of a robust arcuate GABAergic input to gonadotropin-releasing hormone neurons in a model of polycystic ovarian syndrome. *Proc Natl Acad Sci U S A*. 2015;112:596-601. doi:10.1073/pnas.1415038112
23. Dulka EA, Moenter SM. Prepubertal development of gonadotropin-releasing hormone neuron activity is altered by sex, age, and prenatal androgen exposure. *Endocrinology*. 2017;158:3943-3953. doi:10.1210/en.2017-00768
24. Berg T, Silveira MA, Moenter SM. Prepubertal development of GABAergic transmission to gonadotropin-releasing hormone (GnRH) neurons and postsynaptic response are altered by prenatal androgenization. *J Neurosci*. 2018;38:2283-2293. doi:10.1523/JNEUROSCI.2304-17.2018
25. Caligioni CS. Assessing reproductive status/stages in mice. *Curr Protoc Neurosci*. 2009; Supplement 48: Appendix 4:Appendix 4I. doi:10.1002/0471142301.nsa04is48
26. DeFazio RA, Heger S, Ojeda SR, Moenter SM. Activation of A-type gamma-aminobutyric acid receptors excites gonadotropin-releasing hormone neurons. *Mol Endocrinol*. 2002;16:2872-2891. doi:10.1210/me.2002-0163
27. Herbison AE, Moenter SM. Depolarising and hyperpolarising actions of GABA(A) receptor activation on gonadotrophin-releasing hormone neurones: towards an emerging consensus. *J Neuroendocrinol*. 2011;23:557-569. doi:10.1111/j.1365-2826.2011.02145.x
28. Jaime J, Moenter SM. GnRH neuron excitability and action potential properties change with development but are not affected by prenatal androgen exposure. *eNeuro*. 2022;9. doi:10.1523/ENEURO.0362-22.2022
29. Feria Pliego JA, Pedroarena CM. Kv1 potassium channels control action potential firing of putative GABAergic deep cerebellar nuclear neurons. *Sci Rep*. 2020;10:6954. doi:10.1038/s41598-020-63583-7
30. Johnston J, Forsythe ID, Kopp-Scheinpflug C. Going native: voltage-gated potassium channels controlling neuronal excitability. *J Physiol*. 2010;588:3187-3200. doi:10.1113/jphysiol.2010.191973
31. Mendonça PRF, Kyle V, Yeo SH, Colledge WH, Robinson HPC. Kv4.2 channel activity controls intrinsic firing dynamics of arcuate kisspeptin neurons. *J Physiol*. 2018;596:885-899. doi:10.1113/JP274474
32. Storm JF. Action potential repolarization and a fast after-hyperpolarization in rat hippocampal pyramidal cells. *J Physiol*. 1987;385:733-759. doi:10.1113/jphysiol.1987.sp016517
33. DeFazio RA, Moenter SM. Gonadotropin-releasing hormone (GnRH) neuron potassium currents and excitability in both sexes exhibit minimal changes upon removal of negative feedback. *eNeuro*. 2021;8. doi:10.1523/ENEURO.0126-21.2021
34. Suter KJ, Song WJ, Sampson TL, et al. Genetic targeting of green fluorescent protein to gonadotropin-releasing hormone neurons: characterization of whole-cell electrophysiological properties and morphology. *Endocrinology*. 2000;141:412-419.
35. DeFazio RA, Moenter SM. Estradiol feedback alters potassium currents and firing properties of gonadotropin-releasing hormone neurons. *Mol Endocrinol*. 2002;16:2255-2265. doi:10.1210/me.2002-0155
36. Bezanilla F, Armstrong CM. Inactivation of the sodium channel. I. Sodium current experiments. *J Gen Physiol*. 1977;70:549-566. doi:10.1085/jgp.70.5.549
37. Clay JR. Determining K+ channel activation curves from K+ channel currents. *Eur Biophys J*. 2000;29:555-557. doi:10.1007/s002490000091
38. Clay JR. Determining k channel activation curves from k channel currents often requires the Goldman-Hodgkin-Katz equation. *Front Cell Neurosci*. 2009;3:20. doi:10.3389/neuro.03.020.2009
39. Kielland J. Individual activity coefficients of ions in aqueous solutions. *J Am Chem Soc*. 1937;59:1675-1678.
40. Verzani J, Loukides MK, Romano R. *Getting Started with RStudio*. 1st ed. O'Reilly; 2012.
41. Cohen Y, Cohen JY. *1 Online Resource*. Wiley; 2008:619.
42. Pace L. *1 Online Resource*. Apress: Imprint: Apress; 2012:321.
43. Kassambara A. *rstatix: Pipe-Friendly Framework for Basic Statistical Tests. R package version 0.7.2*. 2023 https://rpkgs.datanovia.com/rstatix/
44. Gohel D. *flextable: functions for tabular reporting* (*R package version 0.5.11*). 2020 https://cran.r-project.org/package=flextable
45. Burger LL, Wagenmaker ER, Phumsatitpong C, Olson DP, Moenter SM. Prenatal androgenization alters the development of GnRH neuron and preoptic area RNA transcripts in female mice. *Endocrinology*. 2020;161. doi:10.1210/endocr/bqaa166
46. Chen X, Moenter SM. Gonadal feedback alters the relationship between action potentials and hormone release in gonadotropin-releasing hormone neurons in male mice. *J Neurosci*. 2023;43:6717-6730. doi:10.1523/JNEUROSCI.2355-22.2023
47. Noh W, Pak S, Choi G, Yang S. Transient potassium channels: therapeutic targets for brain disorders. *Front Cell Neurosci*. 2019;13:265. doi:10.3389/fncel.2019.00265
48. Kita T, Kita H, Kitai ST. Effects of 4-aminopyridine (4-AP) on rat neostriatal neurons in an in vitro slice preparation. *Brain Res*. 1985;361:10-18. doi:10.1016/0006-8993(85)91269-7
49. Misonou H. Homeostatic regulation of neuronal excitability by K(+) channels in normal and diseased brains. *Neuroscientist*. 2010;16:51-64. doi:10.1177/1073858409341085
50. Marder E, Prinz AA. Current compensation in neuronal homeostasis. *Neuron*. 2003;37:2-4. doi:10.1016/s0896-6273(02)01173-x
51. Marder E, Goaillard JM. Variability, compensation and homeostasis in neuron and network function. *Nat Rev Neurosci*. 2006;7:563-574. doi:10.1038/nrn1949
52. Shruti S, Clem RL, Barth AL. A seizure-induced gain-of-function in BK channels is associated with elevated firing activity in neocortical pyramidal neurons. *Neurobiol Dis*. 2008;30:323-330. doi:10.1016/j.nbd.2008.02.002
53. Klyachko VA, Ahern GP, Jackson MB. cGMP-mediated facilitation in nerve terminals by enhancement of the spike afterhyperpolarization. *Neuron*. 2001;31:1015-1025. doi:10.1016/s0896-6273(01)00449-4
54. Manis PB. In: Jaeger D, Jung R, eds. *Encyclopedia of Computational Neuroscience*. Springer; 2013:1-16.
55. Du J, Wang Q, Hu F, et al. Effects of estradiol on voltage-gated potassium channels in mouse dorsal root ganglion neurons. *J Membr Biol*. 2014;247:541-548. doi:10.1007/s00232-014-9670-z
56. Gibson AG, Jaime J, Burger LL, Moenter SM. Prenatal androgen treatment does not alter the firing activity of hypothalamic arcuate kisspeptin neurons in female mice. *eNeuro*. 2021;8. doi:10.1523/ENEURO.0306-21.2021
57. Deng P, Pang Z, Zhang Y, Xu ZC. Developmental changes of transient potassium currents in large aspiny neurons in the neostriatum. *Brain Res Dev Brain Res*. 2004;153:97-107. doi:10.1016/j.devbrainres.2004.08.001
58. Nakamura Y, Takahashi T. Developmental changes in potassium currents at the rat calyx of Held presynaptic terminal. *J Physiol*. 2007;581:1101-1112. doi:10.1113/jphysiol.2007.128702

59. Wang W, Gu J, Li YQ, Tao YX. Are voltage-gated sodium channels on the dorsal root ganglion involved in the development of neuropathic pain? *Mol Pain*. 2011;7:16. https://doi.org:10.1186/1744-8069-7-16
60. Shah NH, Aizenman E. Voltage-gated potassium channels at the crossroads of neuronal function, ischemic tolerance, and neurodegeneration. *Transl Stroke Res*. 2014;5:38-58. doi:10.1007/s12975-013-0297-7
61. Köhling R, Wolfart J. Potassium channels in epilepsy. *Cold Spring Harb Perspect Med*. 2016;6. doi:10.1101/cshperspect.a022871
62. Christian CA, Mobley JL, Moenter SM. Diurnal and estradiol-dependent changes in gonadotropin-releasing hormone neuron firing activity. *Proc Natl Acad Sci U S A*. 2005;102:15682-15687. doi:10.1073/pnas.0504270102
63. Adams C, Stroberg W, DeFazio RA, Schnell S, Moenter SM. Gonadotropin-releasing hormone (GnRH) neuron excitability is regulated by estradiol feedback and kisspeptin. *J Neurosci*. 2018;38:1249-1263. doi:10.1523/JNEUROSCI.2988-17.2017
64. DeFazio RA, Navarro MA, Adams CE, Milescu LS, Moenter SM. Estradiol enhances the depolarizing response to GABA and AMPA synaptic conductances in arcuate kisspeptin neurons by diminishing voltage-gated potassium currents. *J Neurosci*. 2019;39:9532-9545. doi:10.1523/JNEUROSCI.0378-19.2019
65. Silva MSB, Desroziers E, Hessler S, et al. Activation of arcuate nucleus GABA neurons promotes luteinizing hormone secretion and reproductive dysfunction: implications for polycystic ovary syndrome. *EBioMedicine*. 2019;44:582-596. doi:10.1016/j.ebiom.2019.05.065
66. Power EM, Ganeshan D, Iremonger KJ. Estradiol regulates voltage-gated potassium currents in corticotropin-releasing hormone neurons. *J Exp Biol*. 2023;226. doi:10.1242/jeb.245222
67. Makkar RR, Fromm BS, Steinman RT, Meissner MD, Lehmann MH. Female gender as a risk factor for torsades de pointes associated with cardiovascular drugs. *Jama*. 1993;270:2590-2597. doi:10.1001/jama.270.21.2590
68. Lehmann MH, Timothy KW, Frankovich D, et al. Age-gender influence on the rate-corrected QT interval and the QT-heart rate relation in families with genotypically characterized long QT syndrome. *J Am Coll Cardiol*. 1997;29:93-99. doi:10.1016/s0735-1097(96)00454-8
69. Argenziano M, Tiscornia G, Moretta R, et al. Arrhythmogenic effect of androgens on the rat heart. *J Physiol Sci*. 2017;67:217-225. doi:10.1007/s12576-016-0459-y
70. Rautaharju PM, Zhou SH, Wong S, et al. Sex differences in the evolution of the electrocardiographic QT interval with age. *Can J Cardiol*. 1992;8:690-695.
71. Masuda K, Takanari H, Morishima M, et al. Testosterone-mediated upregulation of delayed rectifier potassium channel in cardiomyocytes causes abbreviation of QT intervals in rats. *J Physiol Sci*. 2018;68:759-767. doi:10.1007/s12576-017-0590-4
72. Suárez L, Bilal U, Bordallo J, Cantabrana B, Sánchez M. Androgens block outward potassium currents and decrease spontaneous action potentials in GH3 cells. *Naunyn Schmiedebergs Arch Pharmacol*. 2015;388:67-78. doi:10.1007/s00210-014-1057-2
73. Rao VR, Perez-Neut M, Kaja S, Gentile S. Voltage-gated ion channels in cancer cell proliferation. *Cancers (Basel)*. 2015;7:849-875. doi:10.3390/cancers7020813

How to cite this article: Jaime J, DeFazio RA, Moenter SM. Development and prenatal exposure to androgens alter potassium currents in gonadotropin-releasing hormone neurons from female mice. *J Neuroendocrinol*. 2024;36(3):e13373. doi:10.1111/jne.13373